

TRIBOLOGICAL AND CORROSION PROPERTIES OF IRON-BASED ALLOYS

*E. Vernickaite**, *Z. Antar***, *A. Nicolenco* ****, *R. Kreivaitis*****, *N. Tsyntsaru* ****,
H. Cesiulis[†]*

* Vilnius University, Department of Physical Chemistry, Vilnius, Lithuania

** University of Sfax, Materials Engineering and Environment Laboratory, Tunisia

*** Institute of Applied Physics, Chisinau, Moldova

**** Aleksandras Stulginskis University, Institute of Power and Transport Machinery Engineering,
Kaunas, Lithuania

Abstract: Corrosion is responsible for industrial maintenance and industrial accidents costs. A helpful way to prevent corrosion is to develop advanced materials with highly anti-corrosive properties. The electrodeposition is one of the most attractive methods for obtaining these materials. This work deals with evaluation of the tribological and corrosion behaviour of electrodeposited Fe-W and Fe-W-P alloys. Electrodeposits were obtained from 4 different baths and were characterized by means of scanning electron microscopy; X-ray dispersive energy spectroscopy; X-ray diffraction spectroscopy. The hardness was determined by Micro-indentation carried out at normal forces varying from 98 mN up to 980 mN with a loading rate of 1961 mN/min. A ball-disc tribometer was used to study the tribological properties at 90 °C. A diamond indenter, having a radius of 100 µm, was used to carry the scratch test. Corrosion behaviour was studied using polarization and electrochemical impedance spectroscopy technique. It was investigated that in all cases Fe-W and Fe-W-P alloy coatings exhibit greater micro-hardness than the stainless steel substrate. The amorphous-like ternary Fe-W-P alloy coatings demonstrate higher wear and corrosion resistance and lower friction coefficient compared to binary Fe-W alloy coating.

Keywords: iron-based alloys, electrodeposition, tribology, wear, hardness, corrosion.

1. INTRODUCTION

Electrodeposited nanostructured tungsten alloys with iron-group metals are attractive because of tunable mechanical, chemical and magnetic properties, and can be electrodeposited from a number of solutions using various electrodeposition modes [1]. The electrodeposited Fe–W alloys containing higher amount of tungsten are “amorphous-like” and remain nanocrystalline after annealing up to 800 °C. After heating at 1000 °C, the nanocrystalline structure transforms into a microcrystalline one, and three phases are formed, namely FeWO₄, Fe, and possibly Fe₂W [2].

The Fe–W coatings undergo a high degree of wear resulting from the oxidation of the surface and may be considered as alternative to the chromium coatings, which are formed in the hazardous process based on hexavalent chromium [3, 4]. It should be taken into account that features of a sliding system depend on a variety of interrelated mechanical, chemical, physical, and surface properties of materials and surfaces. Tribological behavior largely depends on the crystal structure. When percent of tungsten in iron-group alloys reaches more than 22 at. % its grain size become less than 10 nm, which leads to enhances the hardness of the coating [5]. It has been shown that the nanohardness of as-plated Fe-W with 29 at. % coatings reaches 13 GPa that is comparable to the hardness of electrodeposited chromium [2]. The study of the tribological and mechanical properties of the multilayer Fe-W/Cu coatings by means of electrodeposition leads to the improvement of the wear characteristics of the coatings even at dry friction and at a sufficiently high load of 10 N. Investigations of wear resistance of Fe-W alloy at dry friction and in presence of oil were performed and described in [6]. The specific feature of Co-W and Fe-W alloys under dry friction consists in the formation of oxide layer that results in a faster wear, especially in the case of Fe-W alloys, nevertheless that the W content is similar

[†] Author for contacts: Prof. Henrikas Cesiulis
E-mail: henrikas.cesiulis@chf.vu.lt

in Fe-W and Co-W alloys. The presence of oils substantially decreases oxygen's access to the contact areas and reduces wear of such alloys.

An addition of tungsten in the alloys apparently increases the chemical resistance [7]. This and lower overvoltage for anodic oxidation of methanol in sulfuric acid medium opens perspectives to Fe-W alloys to use its in the fuel cells [8]. It was shown that the presence of tungsten in same binary system results in improvement on corrosion resistance. In the case of Ni-Fe-W alloys, the maximal corrosion resistance is obtained for alloys having tungsten up to 9.2 at. %. However, the charge transfer resistance values of ternary alloy coatings were lower compared to those of the binary alloy coatings due to preferential dissolution of iron from the matrix [9]. These results show that same ternary alloys (Fe-W-Co/Ni) are potential materials for applications in magnetic devices [10]. Also, Fe-W alloys have attracted magnetic properties, electrical resistivity, and reduced films stress that allows using it as new material in micro-/nano-electromechanical systems (MEMS/NEMS) [11].

Recent researches show that the presence of phosphorus in iron alloys influences on tribological properties and its corrosion resistance [12]. The amorphous Ni-W-P alloy with high strength properties was obtained [13, 14]. Introduction of phosphorous into the alloys, for example Co-W, eliminates the cracks even at higher current densities applied for electrodeposition [15].

The aim of this work is to obtain Fe-W and Fe-W-P coatings from different electrolytes and to evaluate their tribological properties and corrosion behaviour.

2. EXPERIMENTAL

The solutions were prepared by dissolving appropriate amounts of chemicals in distilled water and the pH 8.5 was adjusted by additions of concentrated H_2SO_4 . Electrodeposition of thin films was performed at 70 °C temperature in a typical three-electrode cell under direct current mode at 30 mA/cm². A graphite and Ag/AgCl electrode were used as a counter electrode and a reference electrode, respectively. All potential values are expressed versus the Ag/AgCl electrode. The electrodeposition of Fe, Fe-W and Fe-W-P layers were carried out on the stainless steel (Type 304) substrate. Before the experiments the working electrode was rinsed with acetone and 0.1 M H_2SO_4 solution under ultrasound irritation. The thickness of the electrodeposits was calculated from gravimetric and elemental analysis data.

The phase composition and microstructure of the deposited alloys were identified by X-ray diffractometer (XRD, Rigaku MiniFlex II) and scanning electron microscope (SEM, Hitachi TM-3000), supplied with an Oxford EDS analyzer.

Hardness was determined by Micro-indentation (Micro Combi Tester, CSM Instruments) carried out at normal forces varying from 98 mN up to 980 mN with a loading rate of 1961.4 mN/min. The indenter was a Vickers shaped tip with a centreline-to-face angle of 68. A ball-disc tribometer (TRM 500, WAZAU) was used to study the tribological properties at 90 °C. The ball, designed with 100Cr6 steel, have 6 mm diameter. The normal load applied on the contact was about 5 N and average linear velocity was estimated by 0.125 m/s. A diamond Rockwell indenter, having a radius of 100 µm, was used to carry on the scratch test. The wear path was characterized by optical microscopy (Eclipse MA100, Nikon).

Electrochemical corrosion measurements of obtained coatings were performed in the mixture 0.012 M Na_2SO_4 and 0.027 M NaCl (pH 5) at 90 °C. The solution was open to air. The exposed area of the sample was 1 cm². The corrosion tests were performed by means of voltammetry and electrochemical impedance spectroscopy (EIS), recorded at open circuit potential (OCP). The investigations were carried out using AUTOLAB system and GPES and FRA 4.9 software. The registration of EIS and voltammetric data was started after stabilization of the open circuit potential within 15 minutes in the test solution. The amplitude of the modulation potential for the EIS measurements was 5 mV, and the frequency range was 10 kHz-0.01 Hz.

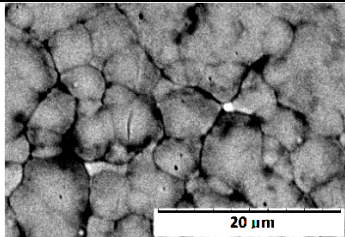
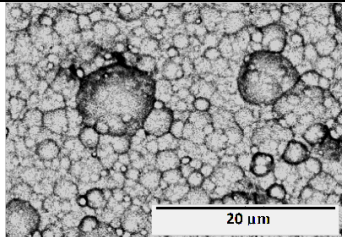
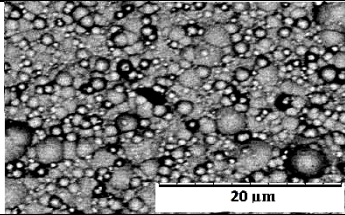
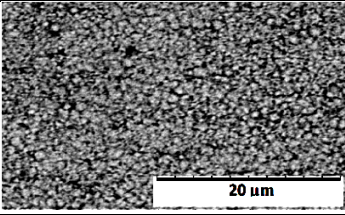
3. RESULTS AND DISCUSSION

Composition and morphology of Fe-alloys. Fe, Fe-W and Fe-W-P thin films were electrodeposited from citrate-containing baths, which compositions are given in Table 1. The SEM images of electrodeposited Fe-W, Fe-W-P alloys and their compositions are shown in Table 2. As it can be seen, the coatings possess micro-granular structure, and Fe-W contains ~25 at. % of W whereas the W content in electrodeposited Fe-W-P alloys contains ~26 at. % of W. Also it was indicated, that wetting and brightening agents presenting in the bath (Bath 4) slightly increases the phosphorous percentage in the deposit. Fe-W and Fe-W-P alloy coatings are uniform and free of cracks. It is clearly seen that even a small amount of phosphorous in the composition (1-1.6 at. %) leads to refining the structure and the deposits become tight, compact and dense.

Table 1. Composition of the baths used for the electrodeposition of Fe-W (Bath 1, 2) and Fe-W-P (Bath 3, 4).

Electrolyte content	Bath 1	Bath 2	Bath 3	Bath 4
Na ₂ WO ₄ ·2H ₂ O (sodium tungstate), M	0.2	0.4	0.4	0.4
FeSO ₄ ·7H ₂ O (iron sulfate), M	0.02	0.2	0.2	0.2
Na ₃ C ₆ H ₅ O ₇ ·2H ₂ O (tri-sodium citrate), M	0.2	0.33	0.33	0.33
C ₆ H ₈ O ₇ ·H ₂ O (citric acid), M	-	0.17	0.17	-
H ₃ BO ₃ (boric acid), M	0.16	-	-	-
H ₂ NaO ₂ P·H ₂ O (sodium hypophosphite), M	-	-	0.02	0.02
H ₃ PO ₄ (phosphoric acid), g/L	7.69	-	-	-
C ₄ H ₁₀ O ₂ (butindiol 1,4), µg/l	-	-	-	50
Wetting agent Rokafenol N-10, µg/l	-	-	-	100

Table 2. The micrographs of as-deposited Fe-W and Fe-W-P alloy coatings.

Composition, in at. %	SEM image	Composition, in at. %	SEM image
Fe-72.7 W-24.3		Fe-74.7 W-25.3	
Bath 1		Bath 2	
Fe-72.1 W-26.8 P-1.11		Fe-72.7 W-25.6 P-1.56	
Bath 3		Bath 4	

Mechanical and tribological properties. Micro-indentation test shows an increase of micro-hardness for all coated sample compared to 304-type stainless steel substrate. The hardest coating was obtained from Bath 2 and had a micro-hardness of 725 HV (Figure 1). Figure 2 shows the evolution of friction coefficient with sliding distance for all prepared coatings. The lowest friction coefficient was recorded for the Fe-P-W sample obtained from Bath 4 (containing wetting and brightening agents) and most of the electrochemically prepared samples presented lower friction coefficients than the 304-type stainless steel substrate.

The scratch test profiles were taken for all deposited samples too. It was noticed that coatings prepared using Bath 1 were the most brittle and cracks spread quickly causing damages on the surface. Samples prepared from Bath 3 and 4 were more stable and the density of cracks is lower (Figure 3). It seems

that phosphorous leads to the formation of more wear resistant coating and enhance the adhesion to the substrate.

Corrosion behaviour. The aim of these experiments was to study the corrosion parameters of pure Fe, Fe-W and Fe-W-P alloy coatings and compare the results to those of 304-type stainless steel. According to the results discussed above, Bath 4 was selected for pure Fe deposition (electrolyte without $\text{Na}_2\text{WO}_4 \cdot 2\text{H}_2\text{O}$ and $\text{H}_2\text{NaO}_2 \cdot \text{H}_2\text{O}$), Fe-W (electrolyte without $\text{H}_2\text{NaO}_2 \cdot \text{H}_2\text{O}$) and Fe-W-P electrodeposition. Electrochemical corrosion measurements of obtained coatings were performed in 0,012 M Na_2SO_4 and 0,027 M NaCl solution (pH 5) at 90 °C. Table 3 presents the SEM micrographs of as deposited Fe, Fe-W and Fe-W-P coatings and morphology of specimens after the corrosion test.

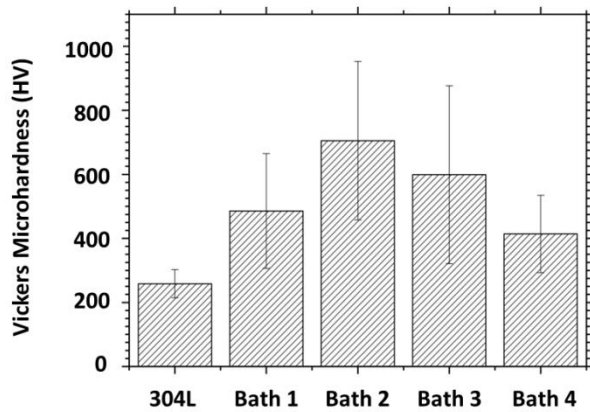


Figure 1. The micro-hardness of as-deposited coatings.

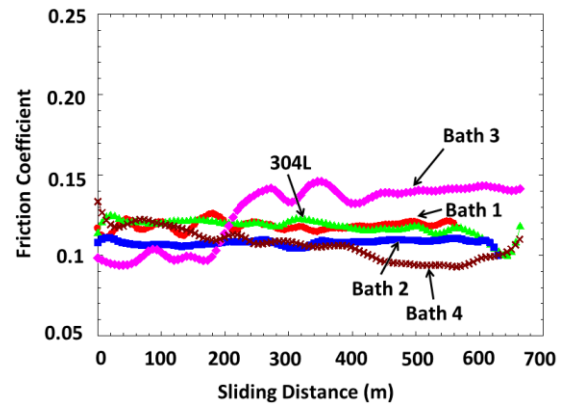


Figure 2. Friction coefficient evolution with sliding distance.

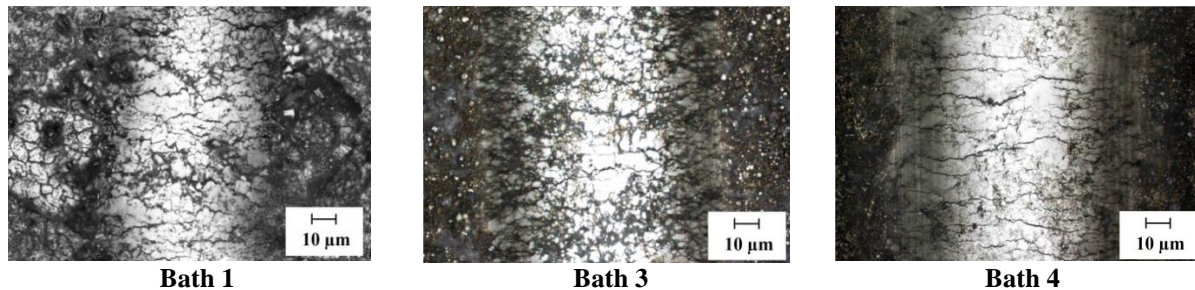
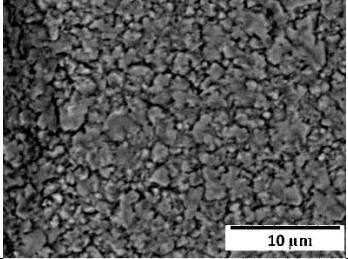
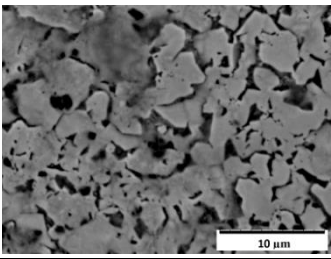
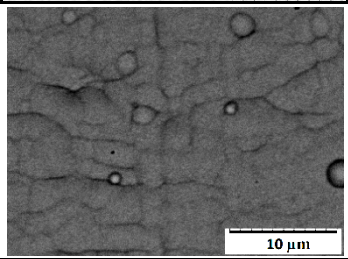
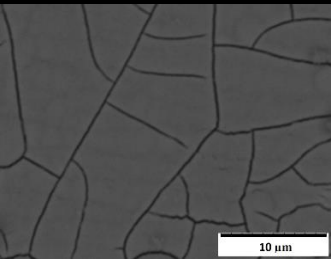
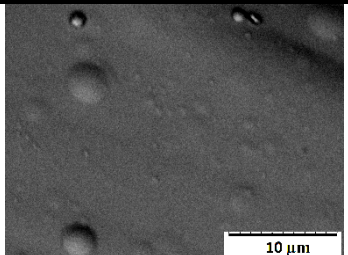
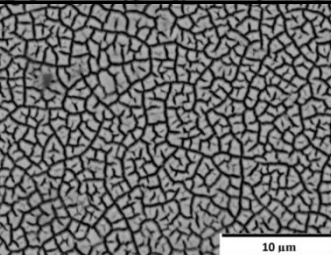


Figure 3. Multi-focus images of the scratch test profiles after exceeding the critical load.

It is seen, that the surface structure after the corrosion experiments in aggressive media significantly changed: granular structure was destroyed and the dense cracks are visible. Investigations also showed that oxygen content in the alloy significantly increases after corrosion experiments.

XRD patterns of as-deposited pure Fe, Fe-W and Fe-W-P alloy coatings are shown in Figure 3. Results indicate that the pure Fe coating exhibit texture with preferred orientation of {211} crystallographic plane. The high content of tungsten in the alloy after electrodeposition causes a significant decrease of grain size and formation of an XRD amorphous-like phase.

Table 3. The micrographs of as-deposited Fe, Fe-W and Fe-W-P alloy coatings. Composition is given in at. %.

<i>As-deposited</i>		<i>After corrosion test</i>	
Composition	SEM image	Composition	SEM image
Fe – 100		Fe – 100	
O - 5.62 Fe - 94.4		O - 22.6 Fe - 77.4	
W - 33.1 Fe - 66.9		W - 46.9 Fe - 53.1	
O - 26.6 W - 41.8 Fe - 31.5		O - 71.1 W - 13.2 Fe - 15.7	
W - 34.5 Fe - 63.9 P - 1.60		W - 33.7 Fe - 60.5 P - 5.81	
O - 23.2 W - 26.4 Fe - 49.2 P - 1.200		O - 68.8 W - 10.2 Fe - 19.5 P - 1.55	

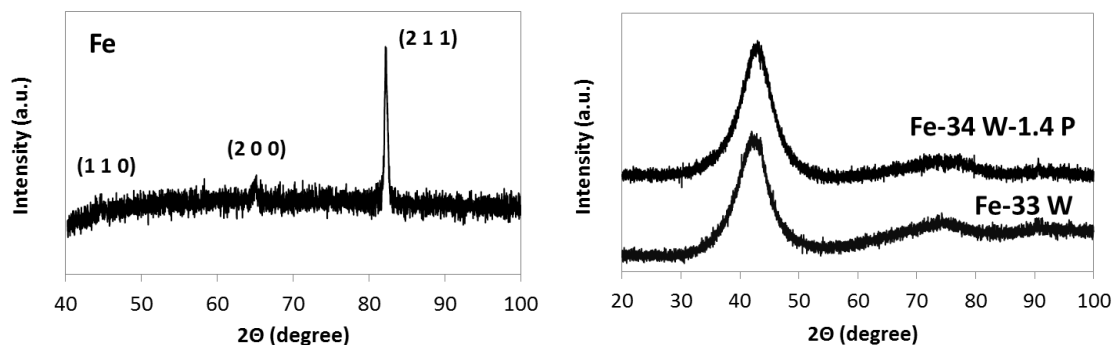


Figure 3. XRD diffraction pattern for pure Fe, Fe-W and Fe-W-P alloy coatings. Composition is given in at. %.

Polarization curves of the specimens tested in 0.012 M Na₂SO₄ and 0.027 M NaCl solution (pH 5) at 90 °C are shown in Figure 4.

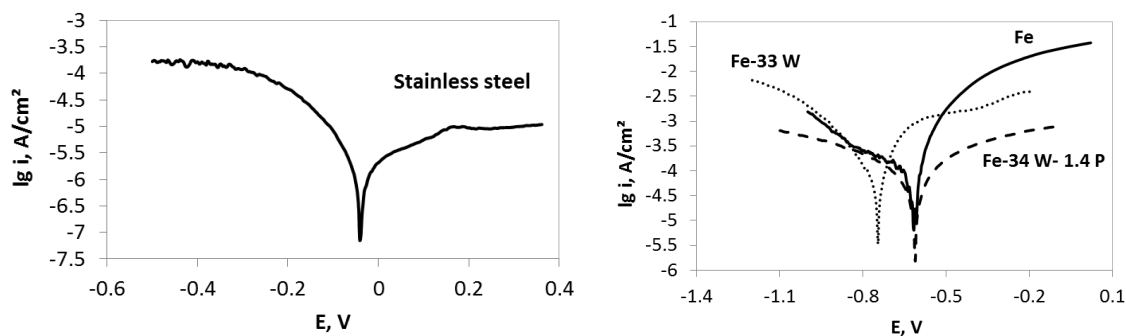


Figure 4. E vs log i plots for 304-type stainless steel, pure Fe, Fe-W and Fe-W-P coatings. Composition is given in at. %.

The polarization curves can be summarised in terms of E_{corr} and i_{corr} , which were calculated using Tafel fit and Allen-Hickling equation, and obtained data is summarized in Table 4. It has been found that adding phosphorous into alloys, and electrodeposited ternary Fe-W-P alloy surface shows nobler E_{corr} and the lowest i_{corr} and thus potentially better corrosion resistance in the tested media.

Table 4. Extracted corrosion parameters from E vs. $\log i$ plots in Figure 4.

Coating	E_{corr} , V	j_{corr} , A/cm ²	R_{corr} , $\Omega \cdot \text{cm}^2$
Stainless steel	-0.039	$9.09 \cdot 10^{-7}$	6567
Fe	-0.616	$3.9 \cdot 10^{-5}$	335.9
Fe-33 W	-0.746	$4.32 \cdot 10^{-5}$	380.7
Fe-34 W-1.4 P	-0.613	$1.81 \cdot 10^{-5}$	388.9

Electrochemical impedance spectroscopy (EIS) data have been obtained in order to investigate the performance of electrodeposited thin films in media containing Cl^- and SO_4^{2-} . Nyquist plots for stainless steel, electrodeposited pure Fe, Fe-W and Fe-W-P coatings are shown in Figure 5. The dots indicated measured data while lines present best-fit data based on electric circuits shown in Figure 6. Impedance data were fitted using different electrical equivalent circuit models to interpret the corrosion resistance processes.

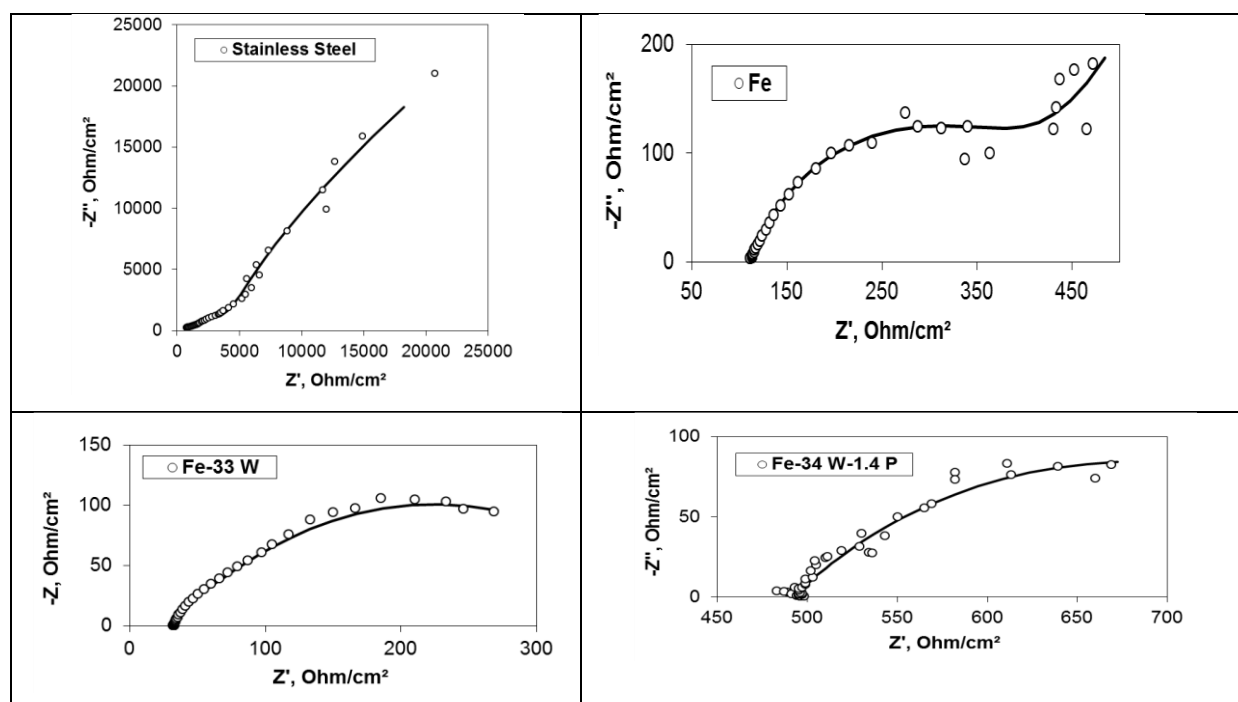


Figure 5. EIS Nyquist plots for stainless steel, pure Co and Fe-W, Fe-W-P alloy coatings in 0.012 M Na_2SO_4 + 0.027 M NaCl (pH 5) solution at OCP. Composition is given in at. %. Equivalent circuit model for stainless steel and Fe-W electrodeposit is given in Figure 6 c; for pure Co – in Figure 6b; for Fe-W-P – in Figure 6 a.

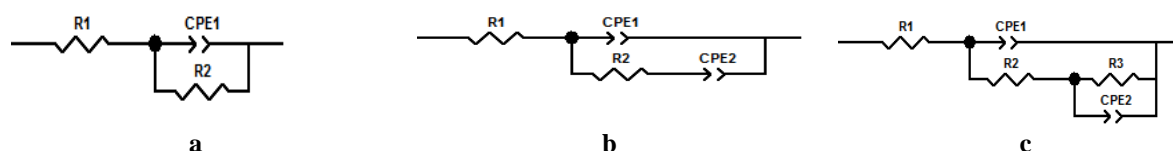


Figure 6. Equivalent circuits of the cell for impedance measurements. R1 - solution resistance; CPE1 - a constant phase element; R2 - charge transfer resistance; CPE2 – the absorption-related constant phase element; R3 – the absorption-related resistance.

R_{corr} values extracted from Nyquist's plots are shown in Table 4. The diameter of medium-frequency capacitive loops is considered as R_{corr} . The ternary Fe-W-P alloy coating demonstrated the higher corrosion resistance than pure Fe and Fe-W electrodeposit. The highest R_{corr} value was obtained for stainless steel substrate. The used equivalent circuit for fitting of EIS data suppose the complicated

mechanism of alloy corrosion involving intermediate stages probably containing adsorbed oxygen compounds; that can explain an increase in oxygen content in the alloys and some changes in tungsten content obtained after corrosion tests.

3. CONCLUSIONS

1. Homogenous and compact Fe-W and Fe-W-P alloy cracks-free coatings containing the high amount of tungsten (24-25 at. %) were deposited from four different plating baths (Table 1). It was indicated that wetting and brightening agents presenting in the plating bath slightly increase the phosphorous percentage in the Fe-W-P deposit. Even a small amount of phosphorous in the composition (1-1.6 at. %) leads to refining the structure.
2. It was found that the hardest Fe-W coating was obtained from Bath 2 and had a micro-hardness of 725 HV. Meanwhile, the lowest friction coefficient was recorded for Fe-W-P sample deposited from Bath 4.
3. Three coatings of pure Fe, Fe-W and Fe-W-P were chosen to evaluate the corrosion behaviour and the results were compared with those of stainless steel. It was found that the Fe-W-P alloy possesses the highest corrosion resistance among pure Fe, and amorphous-like Fe-W. However, cast stainless steel of Type 304 possesses less corrosion current and higher corrosion resistance than deposited Fe-W and Fe-P-W alloys.

ACKNOWLEDGMENT

The authors acknowledge funding from HORIZON2020 SELECTA project (642642) and FP7 Oil&Sugar project (295202). Also, partial funding was granted by the Research Council of Lithuania (MIP-031/2014) and Moldavian national projects (14.02.121A), (14.819.02.16F).

REFERENCES

- [1] N. Tsyntaru, H. Cesiulis, M. Donten, J. Sort, E. Pellicer, E. J. Podlaha-Murphy, *Modern Trends in Tungsten Alloys Electrodeposition with Iron Group Metals*, *Surface Engineering and Applied Electrochemistry*, 48(6), 2012, p. 491-520.
- [2] N. Tsyntaru, J. Bobanova, X. Ye, H. Cesiulis, A. Dikumar, I. Prosycevas, J.-P. Celis, *Iron-tungsten alloys electrodeposited under direct current from citrate-ammonia plating baths*, *Surface and Coatings Technology*, 203, 2009, p. 3136-3141.
- [3] E.W. Brooman, *Wear behavior of environmentally acceptable alternatives to chromium coatings: nickel-based candidates*, *Metal Finishing*, 102(9), 2004, 75-82.
- [4] Zh.I. Bobanova, A.I. Dikumar, H. Cesiulis, J.-P. Celis, N.I. Tsyntaru, I. Prosycevas, *Micromechanical and Tribological Properties of Nanocrystalline Coatings of Iron-Tungsten Alloys Electrodeposited from Citrate-Ammonia Solutions*, *Russian Journal of Electrochemistry*, 45(8), 2009, p. 895-901.
- [5] C. A. Schuh, T. G. Nieh, H. Iwasaki, *The Effect of Solid Solution W Additions on the Mechanical Properties of Nanocrystalline Ni*, *Acta Materialia*, 51, 2003, p. 431-443.
- [6] N. I. Tsyntaru, Zh. I. Bobanova, D. M. Kroitoru, V. F. Cheban, G. I. Poshtaru, A.I. Dikumar, *Effect of a multilayer structure and lubrication on the tribological properties of coatings of Fe-W alloys*, *Surface Engineering and Applied Electrochemistry*, 46(6), 2010, p. 538-546.
- [7] M. Donten, Z. Stojek, J.G. Osteryoung, *Voltammetric, Optical, and Spectroscopic Examination of Anodically Forced Passivation of Cobalt-Tungsten Amorphous Alloys*, *Journal of the Electrochemical Society*, 140(12), 1993, p. 3417-3424.
- [8] C.N. Tharamani, B. Barthasarathi, V. Jayaram, N.S. Begum, S.M. Mayanna, *Studies on electrodeposition of Fe-W alloy for fuel cell application*, *Applied surface science*, 253, 2006, p. 2031-2037.
- [9] K.R. Sriraman, S. Ganesh S. Raman, S.K. Seshadri, *Corrosion behaviour of electrodeposited nanocrystalline Ni-W and Ni-Fe-W alloys*, *Materials Science and Engineering A460-461*, 2007, p. 39-45.
- [10] D. Noce, A.V. Benedetti, M. Magnani, E.C. Passamani, H. Kumar, D.R. Cornejo, C.A. Ospina, *Structural, morphological and magnetic characterization of electrodeposited Co-Fe-W alloys*, *Journal of Alloys and Compounds*, 611, 2014, p. 243-248.
- [11] W. Ehrfeld, V. Hessel, H. Lütwe, Ch. Schulz, L. Weber, *Microsystem Technologies*, 5(3), 1999, p. 105-112.
- [12] J. Nowacki, *Phosphorus in iron alloys surface engineering*, *Journal of Achievements in Materials and*

Manufacturing Engineering, 24(1), 2007, p. 57-67.

[13] J. Ahmad, K. Asami, A. Takeuchi, D.V. Louzguine and A. Inoue, High Strength Ni-Fe-W and Ni-Fe-W-P Alloys Produced by Electrodeposition, Materials Transactions, 44(10), 2003, p. 1942-1947.

[14] E.Valova, S. Armeanov, A. Franquet, K. Petrov, D. Kovacheva, J. Dille, Comparison of the Structure and Chemical Composition of Crystalline and Amorphous Electroless Ni-W-P Coatings, Journal of The Electrochemical Society, 151(6), 2004, C385-C391.

[15] H. Cesiulis, X. Xie, E. Podlaha-Murphy, Electrodeposition of Co-W Alloys with P and Ni, Materials Science, 15(2), 2009, p. 1392-1320.